JOURNAL OF AGRICULTURAL AND FOOD CHEMISTRY

Article

pubs.acs.org/JAFC

# *Trichoderma harzianum* ETS 323-Mediated Resistance in *Brassica oleracea* var. *capitata* to *Rhizoctonia solani* Involves the Novel Expression of a Glutathione S-Transferase and a Deoxycytidine Deaminase

Marthandam Asokan Shibu,[†] Lin Hong-Shin,[†] Yang Hsueh-Hui,[‡,*] and Peng Kou-Cheng*[,†]

[†]Department of Life Science and the Institute of Biotechnology, National Dong Hwa University, Hualien, 97401, Taiwan (ROC)

[‡]Department of Research, Buddhist Tzu Chi General Hospital, General Education Center, Tzu Chi College of Technology, Hualien, Taiwan (ROC)

**ABSTRACT:** Plant interactions with microbial biocontrol agents are used as experimental models to understand resistance-related molecular adaptations of plants. In a hydroponic three-way interaction study, a novel *Trichoderma harzianum* ETS 323 mediated mechanism was found to induce resistance to *Rhizoctonia solani* infection in *Brassica oleracea* var. *capitata* plantlets. The *R. solani* challenge on leaves initiate an increase in lipoxygenase activity and associated hypersensitive tissue damage with characteristic "programmed cell death" that facilitate the infection. However, *B. oleracea* plantlets whose roots were briefly (6 h) colonized by *T. harzianum* ETS 323 developed resistance to *R. solani* infection through a significant reduction of the host hypersensitive tissue damage. The resistance developed in the distal leaf tissue was associated with the expression of a $H_2O_2$-inducible glutathione S-transferase (BoGST), which scavenges cytotoxic reactive electrophiles, and of a deoxycytidine deaminase (BoDCD), which modulates the host molecular expression and potentially neutralizes the DNA adducts and maintains DNA integrity. The cDNAs of *BoGST* and *BoDCD* were cloned and sequenced; their expressions were verified by reverse-transcription polymerase chain reaction analysis and were found to be transcriptionally activated during the three-way interaction.

**KEYWORDS:** *Three-way interaction, deoxycytidine deaminase, glutathione S-transferase, hypersensitive response, lipoxygenase, Trichoderma, Rhizoctonia solani*

## INTRODUCTION

The effects of chemical pesticides that are used in large amounts to control plant pathogens have raised environmental concerns in the last few decades and has prompted the quest for alternatives, such as biocontrol agents (BCAs) and development of genetically modified crops. However, the incomplete understanding of biocontrol mechanisms (BCMs) by which BCAs operate has limited their application and performance. Understanding BCMs will allow the genetic improvement of crops with BCM-associated plant resistance factors, which might both reduce the use of chemical pesticides and prevent the nontarget effects caused by uncontrolled spread of microbial BCAs.[1−3] During the interaction with fungi, plants undergo complex metabolic and physiological changes. Recording the systemic changes during the plant−fungus interaction is important to uncover the physiological or molecular adaptations that help plants to restrict and overcome biotic stress.

*Rhizoctonia solani* is a soil-borne basidiomycete fungus that causes severe damage in economically important crop plants and impacts production globally. The severity of infection differs with members of different anastomosis groups and with the host plant that is being challenged. Plants react to aggressive strains with hypersensitive (HS) response, which usually prevents but in some cases facilitates the fungal penetration into host tissue.[4,5] The *R. solani*-induced lesion formation in cucumber plants is known to be suppressed during host−*Trichoderma* association. But the resistance mechanism developed in the host plant during the interaction is unknown.[6,7]

The plant root colonizing fungi of the species *Trichoderma harzianum* are well-known fungal BCAs that act with a diverse set of unclear, but effective mechanisms to restrict pathogen infection in plants. These mechanisms include antibiosis, direct antagonism over fungal pathogens, and induction of plant systemic and localized resistance.[8−12] Investigations on the plant−*Trichoderma* interaction may enlighten the molecular adaptations and signaling patterns that trigger protection in plants during the interactions with microbes.

*T. harzianum* ETS 323 is well-known for the production of metabolites that are active against plant pathogens. Anthraquinones, L-amino acid oxidase, and glucanases of *T. harzianum* ETS 323 that play a potential role in BCM have been purified and characterized.[13−16] The effect of the interaction of *T. harzianum* ETS 323 with plants on plant resistance has not been studied so far.

In experiments carried out in a custom-designed hydroponic growth (HG) system, the leaves of *Brassica oleracea* var. *capitata* that were challenged with *R. solani* exhibited increased levels of lipoxygenase (LOX) activity, followed by development of HS lesions that spread further to distal parts, making the whole

Received: June 12, 2012
Revised: October 8, 2012
Accepted: October 9, 2012
Published: October 9, 2012





dx.doi.org/10.1021/jf3025634 | *J. Agric. Food Chem.* 2012, 60, 10723−10732

plant susceptible to pathogen colonization. Cabbage plantlets that were preinoculated with *T. harzianum* ETS 323 showed a greater degree of tolerance to the induced stress by restricting the lesion spread and the subsequent *R. solani* infection. *T. harzianum* ETS 323 interaction did not directly affect the systemic LOX activity levels in distal leaves of *B. oleracea* during *R. solani* challenge. The damage protection mechanism in *T. harzianum* ETS 323 colonized plantlets was potentially attributed to two proteins, a glutathione S-transferase (GST) and a deoxycytidine deaminase (DCD) that were found to be induced rapidly and systemically in the distal leaves, which exhibited greater tolerance to the *R. solani* challenge. To our knowledge, no other report is available on the identification of a GST that is induced in the course of a three-way interaction or on any induced DCD in plants.

## MATERIALS AND METHODS

All the chemicals were purchased from (Sigma-Aldrich, St. Louis, MO) unless stated otherwise.

**Fungal Material and Culture Conditions.** *Preparation of T. harzianum ETS 323 Inoculum.* A mycelial plug (4 mm) from an actively growing region of a *T. harzianum* ETS 323 culture was placed in the middle of a fresh potato dextrose agar (PDA, Becton, Dickinson and Co., Sparks, MD) plate. After 48 h of incubation at 27 °C, the spores on the plates were collected by flushing with 2 mL of sterile distilled water. The spore solution was diluted with sterile distilled water and $5 \times 10^4$ *T. harzianum* ETS 323 conidia were used to inoculate 100 mL of potato dextrose broth (PDB, Becton, Dickinson and Co., Sparks, MD). After 24 h of incubation at 27 °C in a shaker (200 rpm) the germinated hyphae were collected by three subsequent centrifugations at 3900*g* for 10 min followed by washing with sterile distilled water. The pellet was suspended in 100 mL of half-strength liquid Murashige and Skoog (MS) medium and used immediately for root interaction studies.

*R. solani Culture on Cellophane Membrane.* A four millimeter diameter *R. solani* plug was placed on the center of a PDA plate on which three centimeter square pieces of cellophane membrane were placed. *R. solani* was incubated for 48 h at 27 °C to allow the mycelium to grow over the cellophane membrane pieces.

**Custom-Designed HG System.** For the three-way interaction studies, *B. oleracea* plantlets were grown in the HG system to allow the simultaneous interaction of *T. harzianum* ETS 323 on roots and of *R. solani* on leaves. The HG system was an opaque base with a large bowl-shaped transparent glass lid, separated by a metal mesh with holes to hang up to 25 2-mL tubes (Labcon, Petaluma, CA). The tubes were filled with MS agar containing 3% sucrose and 1.2% agar. The bottom ends of the tubes were cut so that the root of the seedling grown in the tube could get in contact with the liquid MS medium supplemented with 3% sucrose present in the base of the HG system.

**Plant Growth Conditions and Fungal Interaction Studies.** Healthy seeds of *B. oleracea* were surface sterilized in a solution containing 70% ethanol and 0.1% $HgCl_2$ and thoroughly rinsed several times with sterile water. Seeds were then placed on sterile wet filter paper and incubated in culture bottles containing half-strength MS agar at 4 °C overnight and then at 24 °C for 36 h. After germination, plants were transferred aseptically to MS agar tubes in the HG system and were grown in a growth chamber with a 12 h photoperiod. After 14 days of plant growth, germinated *T. harzianum* ETS 323 spores were inoculated in the medium contained in the base of the HG system to interact with the plant roots that protruded through the tubes. To ascertain the *T. harzianum* ETS 323–*B. oleracea* root association, the roots were stained with a drop of lactophenol aniline blue solution according to the manufacturer's instructions and observed on an inverted microscope (IX70, Olympus, Tokyo, Japan).

After 6 h of interaction, one piece of cellophane membrane covered with *R. solani* mycelium was placed on one leaf of *B. oleracea*. After 12 h of interaction, the whole shoot, except the leaf inoculated with *R. solani*, was collected and frozen immediately in liquid nitrogen.

**Lipoxygenase Assay.** For LOX assay, 100 mg of leaves was homogenized with 1.25 mL of potassium phosphate buffer (100 mM, pH 7) containing 7% polyvinylpolypyrrolidone. The homogenate was mixed with 0.4 mL of 10% Triton X100 and centrifuged at 6000*g* for 15 min. The supernatant was used directly as the enzyme source. LOX activity was measured using the formation of conjugated dienes from linoleic acid. The reaction mixture consisted of 15–20 μL of enzyme extract and 2.9 mL of 0.4 mM linoleic acid in pH 7 potassium phosphate buffer containing 0.1% Tween 20. The rate of change in absorbance was measured at 234 nm (conjugated diene formation) for 10 min using a NanoVue UV/visible spectrophotometer (GE Healthcare Life Sciences, NJ). Each experiment was repeated four times using independent samples. Protein concentrations were determined using the Bradford method.[17]

**DNA Fragmentation Assay.** DNA from distal tissues (4 mm from the *R. solani* plugs) of *B. oleracea* shoots was extracted and analyzed as described previously with slight modifications.[18] Briefly, *B. oleracea* shoots (200 mg) were frozen in liquid nitrogen and ground into a fine powder. The samples were lysed by incubating in 500 μL of 2% CTAB solution [100 mM Tris-HCl, pH 8.0; 1.4 M NaCl; 20 mM Ethylenediaminetetraacetic acid (EDTA); 1% polyvinylpyrrolidone; and 2% (wt $vol^{-1}$) cetyltrimethylammonium bromide] for 15 min at 55 °C. The purified DNA was electrophoresed in a 1% agarose gel and stained in a solution of 0.25 mg $mL^{-1}$ ethidium bromide.

**Protein Extraction and Quantification for 2D Electrophoresis.** Distal leaves were weighed, ground in a mortar with a pestle using liquid nitrogen to a grayish white powder that was washed by mixing with ice-cold methanol (1.5 mL per 100 mg of leaf tissue), treated with a protease inhibitor cocktail (for plant cell extracts) in a concentration of 10 μL $mL^{-1}$, and centrifuged at 16 000*g* at 4 °C. The pellet was washed repeatedly (three or four times) until a clear supernatant was obtained. The pellet was then washed twice with 1.5 mL of ice-cold acetone, dried using a Speedvac centrifugal dryer (Thermo, Scoresby, Victoria, Australia) for 30 s, and suspended in a rehydration buffer containing 9 M urea, 2% 3-[(3-cholamidopropyl)-dimethylammonio]-1-propane sulfonate (CHAPS), 1% dithiothreitol (DTT), and 10 mM phenylmethylsulfonyl fluoride (PMSF). The samples were then centrifuged (30 min, 16 000*g* at 20 °C) and the supernatants were recovered. Protein concentration was determined using the 2D Quant kit (GE Healthcare Life Sciences) as per the manufacturer's instructions.

**Two-Dimensional Electrophoresis.** Isoelectric focusing (IEF) was done using 17 cm immobilized-pH-gradient (IPG) strips (Bio-Rad, Hercules, CA) with a pH range from 4 to 7, rehydrated with the protein sample in a solution containing 8 M urea, 2% CHAPS, 50 mM DTT, and 2% carrier ampholyte (Bio-Rad). Two hundred micrograms of respective protein sample was loaded in the focusing tray and allowed to be absorbed into the gel strip (12 h actively with a 50 V current). IEF was performed in the PROTEAN IEF Cell system (Bio-Rad). IPG strips were focused up to a total of 14 kV h by using a three-step program (250 V for 1 h, 4 kV for 3 h, and until 10 kV h was reached). The strips were equilibrated in a solution of 6 M urea, 0.375 M Tris/HCl (pH 8.8), 2% sodium dodecyl sulfate (SDS), 20% glycerol, and 2% DTT for 15 min and then for 15 min in 6 M urea, 0.375 M Tris/HCl (pH 8.8), 2% SDS, 20% glycerol, 2.5% iodoacetamide. For the second dimension separation, the strips were positioned on 1 mm thick SDS polyacrylamide gels (10%) and sealed with 1% agarose. The gels were run on the PROTEAN II system (Bio-Rad) at 24 mA $gel^{-1}$ until the bromophenol blue dye front moved down to the end of the SDS gel.

**Protein Visualization and Image Analysis.** Silver staining of gel compatible with mass spectrometry was performed following the method described by Gharahdaghi et al. with slight modification.[19] Gel was fixed for 30 min in 50% methanol and 10% acetic acid, followed by 15 min in 50% methanol, and 5 × 5 min repeated water washes. Gel was then sensitized for 1 min in 0.02% sodium thiosulfate, followed by 2 × 1 min water washes, and incubated for 25 min in 0.2% silver nitrate. After two quick water washes, proteins were visualized with developing solution (3% sodium carbonate, 0.025% formalin), and the reaction was stopped with 1.4% EDTA.

**In-Gel Digestion and ESI-QUAD-TOF.** Protein spots from the preparative gel were manually excised into 1 × 1 mm pieces and washed for 15 min at 27 °C in a solution containing 20 μL of 30 mM potassium ferricyanide and 20 μL of 100 mM sodium thiosulfate. The gel pieces were washed three times with 100 μL of 25 mM ammonium bicarbonate for 10 min and then for 10 min with 25 mM ammonium bicarbonate in acetonitrile (1:1, v/v). The gel pieces were then vacuum-dried in a Speedvac. Proteins in the gel pieces were reduced for 1 h with 40 μL of 10 mM DTT in 25 mM ammonium bicarbonate at 56 °C and alkylated in the dark for 45 min with 40 μL of 55 mM iodoacetamide in 25 mM ammonium bicarbonate at 27 °C. After a 15 min wash with 100 μL of 25 mM ammonium bicarbonate in acetonitrile (1:1, v/v), the gel pieces were dehydrated in 100 μL of acetonitrile for 5 min and dried by the Speedvac. Proteins were digested with 0.01 μg $mL^{-1}$ of trypsin (Promega, Annandale, NSW, Australia) in 25 mM ammonium bicarbonate for 16 h at 37 °C. After digestion, the protein suspension was collected as a supernatant after centrifugation at 10 000*g* for 10 min. Further, the sample was incubated in 20 μL of 5% formic acid in acetonitrile (1:1, v/v) for 20 min and centrifuged at 12 000*g* for 10 min to collect the supernatant. The extract was dried by the Speedvac, and peptides were suspended in 20 μL of 0.1% formic acid.

The digested peptides were separated and analyzed by a nanoscale LC using an Ultimate capillary LC system (LC-Packings, San Francisco, CA), coupled to a quadrupole time-of-flight mass spectrometer (QSTAR XL, Applied Biosystems, CA) as described previously.[20] Peptide mass fingerprint (PMF) data were analized for matches in the National Centre for Biotechnology Information (NCBInr) database using the Mascot online software tool (Matrix Science, London, UK). Default parameters were used and submitted to the database search program MASCOT (version 2.1 or 2.2, Matrix Science). Search parameters were as follows: peptide and fragment mass tolerances 2 and 0.8 Da, respectively; carbamidomethyl (C), oxidation (M) specified as variable modification; enzyme specificity was trypsin; and one missed cleavage was allowed.

**Semiquantitative Reverse-Transcription Polymerase Chain Reaction (RT-PCR).** Total RNA was extracted from 100 mg of tissue from distal leaf samples using the TRIzol reagent (Invitrogen, Carlsbad, CA) according to the manufacturer's instructions. After quantification, 1.5 μg of RNA was reverse transcribed using the Superscript III kit (Invitrogen). Semiquantitative RT-PCR was performed for appropriate cycles at 94 °C for 15 s, 50 °C for 30 s, and 72 °C for 30 s using the primers 5′-ATGGCAGGTAT-CAAAGTTTTC-3′ and 5′-TCACTGAAGGATCTTCTGG-3′ for *GST*, and 5′-ATGGAAGAAGCTAAAGTGGAA-3′ and 5′-TCAGTA-TAAACGGAACTTCTCCTTGGT-3′ for *DCD*, and 5′-TCCATCTTGGCATCTCTCAG-3′ and 5′-GTACCCGCATCAGG-CATCTG-3′ for *Actin*.

**Sequence Analysis.** The amplified cDNA were ligated into PCR 2.8 vector by using the TOPO TA cloning kit (Invitrogen) and the inserts were sequenced by the commercial sequencing service provided by the Protech Technology Enterprise Co., Ltd., Taipei, Taiwan (Republic of China). Multiple sequence alignment and phylogenetic tree were made using the online Clustal X tool in the EMBL-EBI web server by the neighbor-joining method.

## RESULTS

Microscopic observations on the hydroponic roots of plantlets cocultured with *T. harzianum* ETS 323 showed that germinated *T. harzianum* ETS 323 hyphae recognized and colonized the plant roots densely within 6 h after inoculation (Figure 1A). *T. harzianum* ETS 323 that colonized hydroponic roots developed lateral hyphal structures that can be interpreted as accelerated morphological changes in response to plant association within 6 h of hydroponic interaction (Figure 1B). *T. harzianum* ETS 323 colonizing a nylon fiber was used as control. *T. harzianum* ETS 323 colonization of nylon fibres was scarce, and no morphological change was observed 6 h after inoculation (Figure 1C,D).

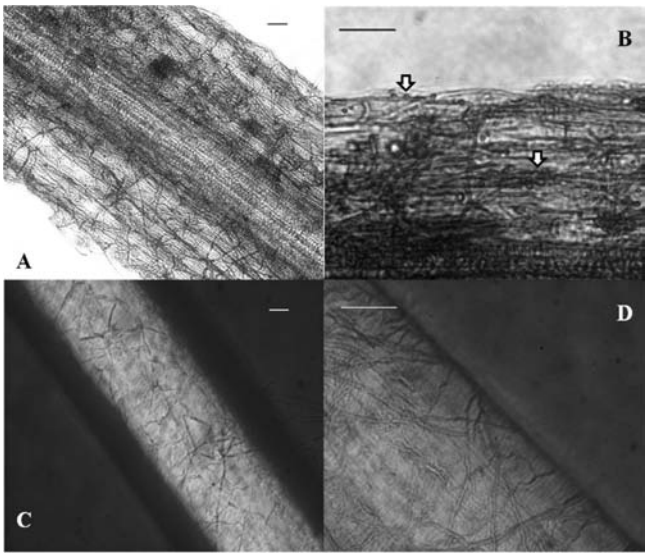


**Figure 1.** Microscopic pictures of *Trichoderma harzianum* ETS 323 colonizing in *B. oleracea* var. *capitata* roots 6 h after inoculation with germinated hyphae. (A) *B. oleracea* root colonized by *T. harzianum* ETS 323. (B) Dense mycelial network on the root surface. (C, D) *T. harzianum* ETS 323 colonizing nylon fibers used as control. Arrows indicate lateral hyphal structures that developed 6 h after inoculation. Scale bar represents 50 μm.

**Effect of Three-Way Interaction on the LOX Activity.** The immediate effect on the local and systemic LOX activity in host plantlets treated with *R. solani* (PR), *T. harzianum* ETS 323 (PT), *T. harzianum* ETS 323 and *R. solani* (PTR), or 16 mM $H_2O_2$ (PH) were comparatively analyzed in comparison with untreated control plantlets (P). Periodic examination of LOX activity in the inoculated leaves (local leaves) and distal leaves of *B. oleracea* plantlets showed that *R. solani* interaction steadily increased the active LOX enzyme levels. After 6 h of *R. solani* challenge, plantlets of the PR test group showed a 3-fold increase in LOX activity measured in local leaves. The activity further increased 13-, 18-, and 24-fold within 12, 24, and 48 h, respectively (Figure 2, lLOXPR). The systemic LOX activity that was measured in the distal leaves of the PR test group showed a 50% increase within 6 h of challenge, which further increased up to 4-, 12-, and 15-fold within 12, 24, and 48 h, respectively (Figure 2, sLOXPR). Conversely, in the PT group plantlets, the localized LOX activity measured in the roots showed only a 9-fold increase in 24 h (Figure 2, lLOXPT). The systemic LOX activity in PT group plantlets did not show any significant increase (Figure 2, sLOXPT). The PTR group plantlets showed a substantial increase in LOX activity in the distal leaves, with a pattern comparable to that of PR (Figure 2, LOXPTR). These results suggest that the *R. solani* challenge induces a rapid and substantial increase of LOX activity levels in plantlets of *B. oleracea*, whereas *T. harzianum* ETS 323 colonization induces a limited increase in LOX activity.

**Effect of Three-Way Interaction on DNA Integrity.** DNA integrity in the distal parts of *B. oleracea* was observed to decline within 12 h of *R. solani* challenge. The nuclear DNA of *B. oleracea* run on an agarose gel showed bands and smears that represented fragmented nuclear DNA (Figure 3, L2). The DNA integrity, however, in the distal tissues of PTR group remained unaltered (Figure 3, L3). This shows that in a three-

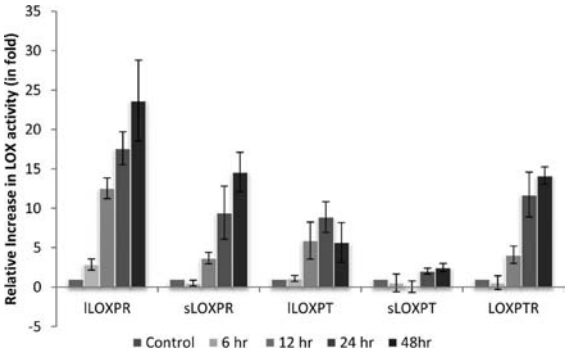


**Figure 2.** Effect of *R. solani* and *T. harzianum* ETS 323 interactions on the local and systemic lipoxygenase (LOX) activity of *B. oleracea* var. *capitata*. The results show the relative normalized levels of LOX activity compared to the control group (P) values made equal to 1. lLOXPR and sLOXPR represent respectively the local and systemic LOX activity measured in leaves of *B. oleracea* challenged with *R. solani* (PR). lLOXPT and sLOXPT represent respectively the local and systemic LOX activity measured in leaves of *B. oleracea* plantlets colonized by *T. harzianum* ETS 323 (PT). LOXPTR indicates LOX activity in the distal leaves of *B. oleracea* plantlets colonized by *T. harzianum* ETS 323 during *R. solani* challenge (PTR). Error bars indicate standard error of the mean ($n$ = 4).

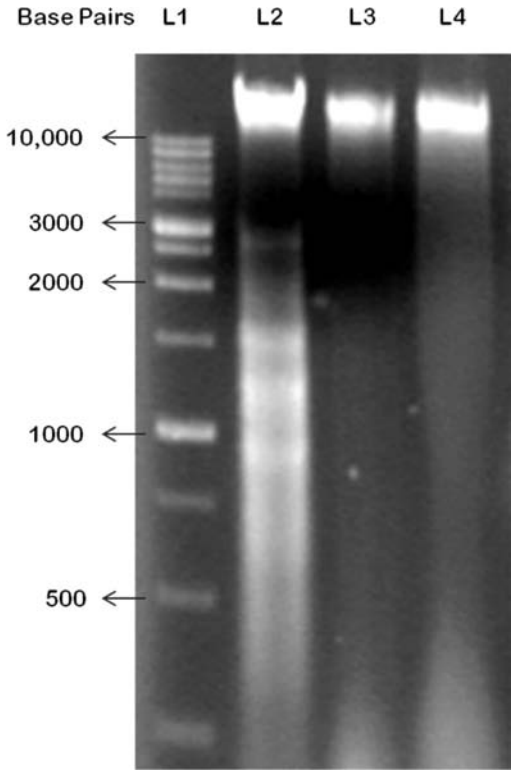


**Figure 3.** Effect of *T. harzianum* ETS 323 inoculation on the DNA fragmentation associated with *R. solani* infection of *B. oleracea* var. *capitata*. Root colonization with *T. harzianum* ETS 323 protected the DNA integrity in the distal tissues of *B. oleracea* during the subsequent *R. solani* challenge: (L1) DNA marker; nuclear DNA from distal tissues of *B. oleracea* (L2) 12 h after *R. solani* challenge (PR); (L3) 18 h after *T. harzianum* ETS 323 root colonization (PT); and (L4) 12 h after *R. solani* challenge of plants pretreated (6 h) with *T. harzianum* ETS 323 (PTR).

way interaction the DNA fragmentation activated in response to *R. solani* challenge was inhibited. As expected, the DNA integrity in the PT test group remained unchanged (Figure 3, L4).

**Effect of Three-Way Interaction on Lesion Proliferation.** After 24 h of *R. solani* challenge, the PR test group leaves developed lesions that covered the entire leaf and further spread to the neighboring leaves within 4 days (Figure 4B). On the contrary, in the PTR group plantlets, the lesions developed on the local leaves were comparatively smaller and limited to 3−4 mm in diameter even after 4 days of *R. solani* challenge (Figure 4C). The PTR leaf lesions did not spread further to the neighboring leaves. This shows that the plantlets in the three-way interaction developed resistance against *R. solani*. The control leaves from P group and PT group plantlets remained healthy (Figure 4A,D).

**Effect of the Three-Way Interaction on Host Susceptibility to *R. solani*.** The plantlets with lesions that spread to the whole leaf were considered susceptible, since these lesions subsequently spread to the entire plantlet. The plantlets with lesions restricted to 3−4 mm were considered resistant, since the infection was arrested and the plants survived. Within 4 days of *R. solani* challenge, all the PR group plantlets tested were found to be susceptible, whereas 87% of the PTR group plantlets in the three-way interaction survived (Figure 5). This result shows that the root colonization by *T. harzianum* ETS 323 in the three-way interaction induced resistance to the *R. solani*. All 50 plantlets in the PT and P groups used as control were healthy.

**Resistance Related Proteins Induced Due in the Three-Way Interaction.** To investigate the possible regulatory mechanism of resistance of PTR group plantlets to *R. solani*, proteins that were induced during the three-way interaction were identified by the two-dimensional protein profile of distal leaves of PTR, PT, PR, PH, and P test group plantlets. The distal leaves were taken into account since the highest resistance to HR tissue damage was observed in distal leaves of the PTR group plantlets. Two interesting protein spots (spots 1 and 2) in the PTR test group proteome were observed to be induced exclusively after the three-way interaction (Figure 6). Spot 1 was also induced in the proteome of PH group plantlets treated with 30 mM $H_2O_2$ (Figure 6). The induced proteins were identified from their trypsin-digested peptide mass fingerprints as a ∼24 kDa glutathione S-transferase (GST, EC 2.5.1.18) and a ∼ 20 kDa deoxycytidine deaminase (DCD, EC 3.5.4.14) by using an online MASCOT similarity search. The GST was found to be homologous to glutathione S-transferase 2 (Genbank protein accession AAP58392) from *Brassica juncea* and the DCD was homologous to a phi class deoxycytidine deaminase (Genbank protein accession AAL67435) from *B. oleracea* (Figure 7). The established functional annotations of these proteins, such as detoxification of cytotoxic reactive electrophile species (RES), modulation of gene expression, and enhanced metabolism, may contribute to the resistance observed in the PTR group plantlets.

**Determination of Transcriptional Patterns of the Induced Proteins.** The transcriptional activation of the GST and DCD was verified by RT-PCR analysis. Both proteins were expressed in the resistant distal leaves in the PTR group plantlets but not in the PR, PT, or P (control) groups. However, GST expression was induced also by 30 mM $H_2O_2$ (Figure 8). The results show that the mRNA expression correlates with the protein expression patterns.

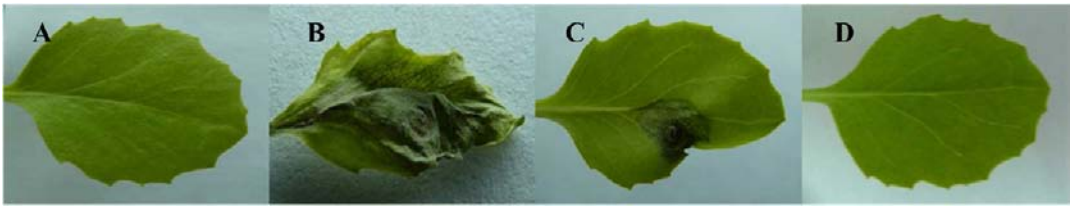


**Figure 4.** Effect of *T. harzianum* ETS 323 interaction on the severity of the lesions formed on *B. oleracea* var. *capitata* leaves in response to 4 days of *R. solani* challenge. Lesions in PR groups spread all over the leaf within 4 days. (A) Control leaf without *R. solani* challenge or *T. harzianum* ETS 323 root colonization (P). (B) Lesion of leaf challenged with *R. solani* (PR). (C) Attenuated lesion of leaf challenged with *R. solani* in a plantlet treated with *T. harzianum* ETS 323 (PTR). (D) Leaf of plantlet colonized by *T. harzianum* ETS 323 (PT).

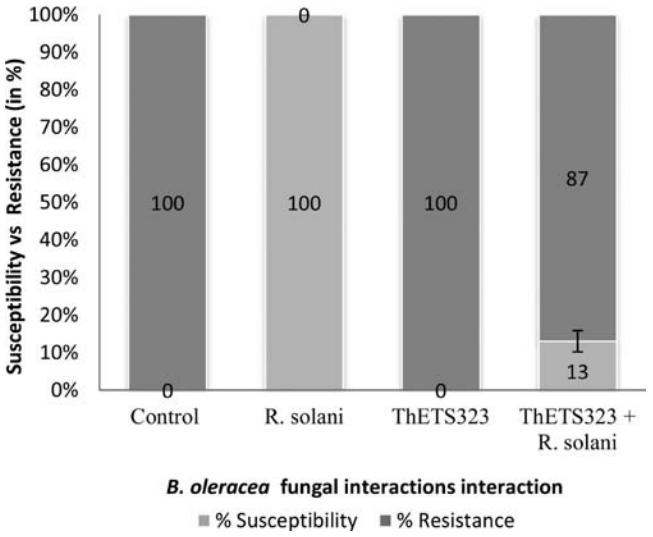


**Figure 5.** Effect of the *T. harzianum* ETS 323 (*Th*ETS323) interaction on the susceptibility of *B. oleracea* var. *capitata* to *R. solani* on day 4 of challenge. All the *B. oleracea* plantlets inoculated with *R. solani* (two-way interaction) showed lesion spread within 4 days of challenge. Conversely, 87% of the plantlets pretreated with *T. harzianum* ETS 323 (three-way interaction) showed resistance to *R. solani*. Error bars indicate standard error of the mean ($n$ = 4).

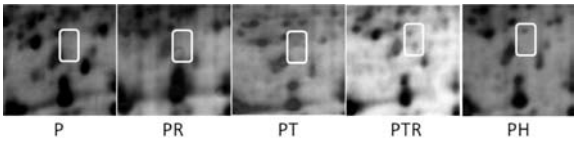


**Figure 6.** Details of two-dimensional gels of the proteome of distal leaves of *B. oleracea* var. *capitata* that show the glutathione S-transferase (BoGST) and deoxycytidine deaminase (BoDCD) expression resulting from different treatments. The marked boxes in P (control leaves), PR (distal leaves of *R. solani*-challenged plantlets), and PT (leaves of plantlets that were colonized by *T. harzianum* ETS 323) show the absence of BoGST and BoDCD spots in the respective proteome. The boxed spots in PTR (distal leaves of *R. solani*-challenged plantlets that were colonized by *T. harzianum* ETS 323) are BoGST and BoDCD during three-way interaction. The boxed spots in PH (leaves of plantlets treated with 30 mM hydrogen peroxide) are the induced BoGST, which was also expressed in PTR group.

**Cloning and Sequence Analysis of the Induced *GST* and *DCD*.** The cDNAs obtained from reverse transcription of total mRNA was amplified with specific primers of *GST* and *DCD* that were designed by considering the MOSCOT results of the proteins. Full-length DNA molecules of 642 and 558 bp, with an open reading frame starting with an ATG start codon and ending with a stop codon, were obtained and named as the

**Sequence 1**

*MAGIKVFGHAASTATRRVLLTLHEKNLDFELVHVELKDGEHKKEPFLSRNP

FGKVPAFEDGDLKLFESRAITQYIAHRYEEEGTNLLPADSKNISHYAIMAIGM

EVEAHHFDPVASKLAWEQVFKLFYGMTTDQAVVEEEEAKLATVLDVYEAR

LKEFKYLAGETFTLTDLHHIPVIQYLLGTPTKKLFDERPHVSEWVAEITNRPAS

QKILQ

**Sequence 2**

*MEEAKVEAKDGTISVATAFAGHQQAVQDSDHKFLTQAVEEAYKGVDCGD

GGPFGAVIVHKNEVVASCHNMVLKYTDPTAHAEVTAIREACKKLNQIELSEC

EIYASCEPCPMCFGAIHLSRLKRLVYGAKAEAAIAIGFDDFIADALRGTGVYQ

KSNLEIKKADGNGAAIAEQVFQNTKEKFRLY

**Figure 7.** MOSCOT search results for the ESI-LC−MS maps of the two protein spots (spots 1 and 2) induced in the distal leaves of *Brassica oleracea* var. *capitata* plantlets indicate that they are glutathione S-transferase (GST) and deoxycytidine deaminase (DCD), respectively. Sequence 1: amino acid sequence of the homologous GST from *B. juncea* (mustard). Sequence 2: amino acid sequence of the homologous DCD from *B. oleracea* (cauliflower). The fragments that denote homology are shaded in gray.

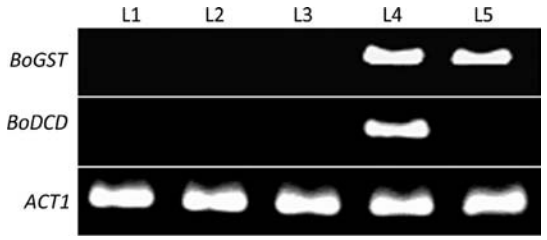


**Figure 8.** RT-PCR analysis of the systemic expression of *B. oleracea* var. *capitata* glutathione S-transferase (*BoGST*) and *B. oleracea* deoxycytidine deaminase (*BoDCD*) transcripts during fungal interactions: L1, control *B. oleracea* plantlets (P); L2, *R. solani*-challenged (12 h) plantlets (PR); L3, *T. harzianum* ETS 323 root colonized (18 h) plantlets (PT); L4, *R. solani*-challenged (12 h) and *T. harzianum* ETS 323 root colonized (18 h) plantlets; and L5, hydrogen peroxide (30 mM) treated (2 h) plantlets (PH). *BoGST* and *BoDCD* expression was induced in distal leaves of *T. harzianum* ETS 323 colonized *B. oleracea* plantlets when challenged with *R. solani*. *BoGST* was also expressed in *B. oleracea* plantlets when treated with hydrogen peroxide. The mRNA level of actin1 (*ACT1*) was used as the internal control.

*B. oleracea* var. *capitata GST* (*BoGST*) and *DCD* (*BoDCD*), respectively. Comparison of the *BoGST* with other cDNA counterparts using the Blastp suit revealed that the *BoGST* is similar to *BjGSTF1* in mustard. Therefore *BoGST* (Genbank nucleotide accession JN656712) is proposed as the cabbage

ortholog of *BjGSTF1*. Like other identical plant GSTs, the *BoGST* exhibits two conserved amino acid sequences, GST_NTER (soluble glutathione S-transferases N-terminal domain) and GST_CTER (soluble glutathione S-transferases C-terminal domain), between amino acid positions 2−83 and 93−213 (Figure 9a,b). Similarly, *BoDCD* (Genbank nucleotide accession JN993702) nucleotide sequence was found to be similar to *DCTD1* in cauliflower and exhibits a conserved DCMP_DEAMINASES (cytidine and deoxycytidylate deaminases zinc-binding region), as in other similar plant DCDs, at position 80−117 (Figure 10a,b).

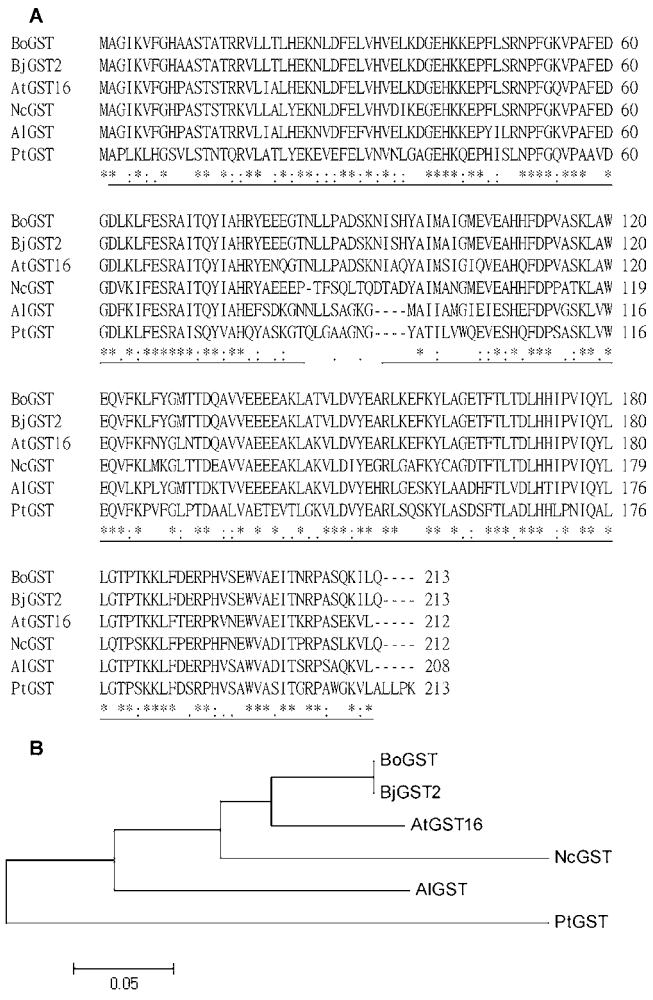


**Figure 9.** (a) Multiple sequence alignment of different plant glutathione S-transferases (GSTs) with the amino acid sequence deduced from the cDNA of *B. oleracea* var. *capitata GST* (*BoGST*), using Clustal W2. The two conserved domains of most GSTs—GST_NTER (soluble glutathione S-transferases N-terminal domain) at position 2−83 and GST_CTER (soluble glutathione S-transferases C-terminal domain) at position 93−213—are underlined. The GST amino acid sequence used for alignment were *B. juncea* BjGST2 (AAP58392), *Arabidopsis thaliana* AtGST16 (NP_178394), *Noccaea caerulescens* NcGST (AAY86772), *Arabidopsis lyrata* AlGST (XP_002892137), and *Populus trichocarpa* PtGST (ADB11333). An asterisk (*) indicates a column with the same amino acid; a colon (:) indicates a column with different amino acids, but highly conserved; and a period (.) indicates a column with different amino acids, but still conserved. A blank indicates a column with dissimilar amino acids or gaps. (b) Phylogenetic tree of different plant GSTs. The GST amino acid sequences used for alignment with BoGST were BjGST2 (AAP58392), AtGST16 (NP_178394), NcGST (AAY86772), AlGST (XP_002892137), and PtGST (ADB11333).

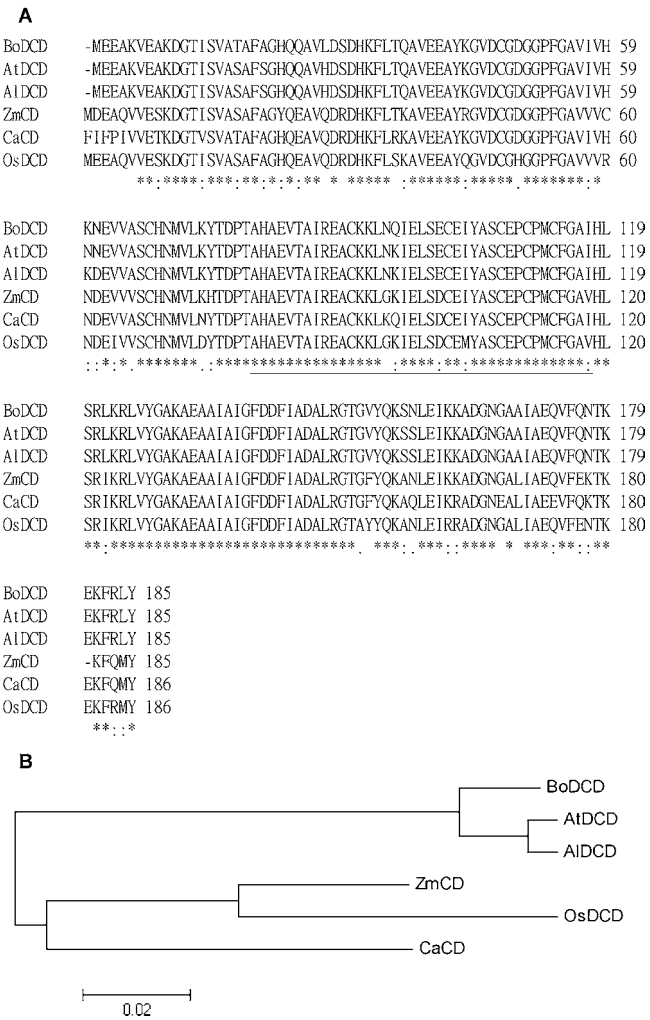


**Figure 10.** Multiple sequence alignment of different plant deoxycytidine deaminases (DCDs) with the amino acid sequence deduced form the cDNA of *B. oleracea* var. *capitata DCD* (*BoDCD*), using Clustal W2. The conserved domain in zinc-binding DCDs DCMP_DEAMINASES (cytidine and deoxycytidylate deaminases zinc-binding region) at position 80−117 is underlined. The DCD amino acid sequence used for alignment were *A. thaliana* AtDCD (NP_198157), *A. lyrata* AlDCD (XP_002874416), *Zea mays* ZmCD (NP_001140513), *Cicer arietinum* CaCD (CAA07230), and *Oryza sativa* OsDCD (NP_001051813). An asterisk (*) indicates a column with the same amino acid; a colon (:) indicates a column with different amino acids, but highly conserved; and a period (.) indicates a column with different amino acids, but still conserved. A blank indicates a column with dissimilar amino acids or gaps. (b) Phylogenetic tree of different plant DCDs. The DCD amino acid sequences used for alignment with BoDCD were AtDCD (NP_198157), AlDCD (XP_002874416), ZmCD (NP_001140513), CaCD (CAA07230), and OsDCD (NP_001051813).

## DISCUSSION

***T. harzianum* ETS 323−Root Interaction.** The interaction between *Trichoderma* and plants has long been studied and the *Trichoderma* root colonization is a well-known phenomenon that initiates various BCMs that are not limited to direct mycoparasitism but also involve the induction of plant

systemic defense response.[21,22] *Trichoderma* hyphae are also known to invade the root epidermis and colonize the intercellular spaces of plant roots up to the cortex layer without causing any tissue damage.[22] The time required to establish a stable root association has not been clearly determined, so far. Previously, germinated hyphae of *T. harzianum* CECT 2413, a plant growth promoting strain, were reported to colonize extensively the entire tomato root within 24 h of coculture and to show increasing morphological changes, such as the formation of lateral papilla-like structures in the root apex within 10 h of interaction.[23] Comparatively, *T. harzianum* ETS 323 was found to be much more active, since this isolate was able to colonize plant roots hydroponically in a relatively shorter time and was shown to undergo morphological changes immediately after inoculation and at a fast rate.

***R. solani* Challenge Induces Elevation of Systemic LOX Activity That Is Unaffected by the Three-Way Interaction.** While LOX is a key enzyme in the synthesis of jasmonic acid that is associated with induced systemic resistance, it is also the key oxidant enzyme for the production of hydroperoxides from fatty acids.[24] Expression of LOXs has been reported in response to biotic stress and has been related to incompatible interactions and HS response in different plants.[25−28] The LOX related lipid hydroperoxides are sources of RES that bind to cellular nucleophiles, particularly to those in peptides and nucleic acids. An unregulated increase in the level of hydroperoxides leads to serious tissue damage.[29,30] An earlier report shows that, when subjected to various biotic stresses, *B. oleracea* leaves show a rapid expression of *BoLOX*, a *LOX* transcript, both locally and systemically.[31] Assuming that the increase in LOX activity in *R. solani*-challenged PR and PTR groups corresponds to increase in LOX products, an increase in LOX-related HS tissue damage is an anticipated consequence.

**Plant Root Interaction with *T. harzianum* ETS 323 Restricts *R. solani*-Induced HS Tissue Damage.** The *R. solani* challenge in leaves of the PR group plantlets resulted in HS tissue damage that was characterized by DNA fragmentation and lesion proliferation. *R. solani* infections are well-known to initiate HS damage that appears rapidly, even before fungal penetration.[32] Plants generally respond to such interaction with an impressive battery of defense mechanisms that form efficient structural and chemical barriers. Moderate stress on plants stimulates cells to express cell survival proteins and thereby to be prepared for subsequent challenges. However, acute or extreme stress, such as that occurring during incompatible interactions, causes damage that often leads to senescence, apoptosis, or necrosis.[33−37] The HS damage during *R. solani* challenge is known to be caused by diffusible elicitors released as a consequence of pathogen's activity. Therefore, it is not restricted to the site of penetration but also spreads to the neighboring tissues.[32] Hypersensitivity restricts the spread of biotrophs, but in the case of necrotrophs like *R. solani*, HS response facilitates the invasion of plant tissue. During the *R. solani* infection, the HS damage with features of programmed cell death (PCD) generally denotes the susceptibility of the host plants to the infection.[38] Therefore, the control of HS tissue damage in the PTR group plantlets actually indicates the development of resistance. In the PTR group, the HS tissue damage is controlled in spite of increased LOX activity. This suggests that the levels of cytotoxic molecules that increase as a consequence of LOX activity are subsequently regulated by a protective mechanism developed in the plantlets.

Numerous reports are available on *R. solani* control by *Trichoderma* in various plant hosts.[6,15,39,40] In cucumber plants, *T. harzianum* SQR-T37 is known to control *R. solani* damping-off disease mainly by mycoparasitism.[6] *R. solani* control by *T. harzianum* ETS 323 seems to be different as the BCM involves the alleviation of HS tissue damage that precedes the *R. solani* infection. This makes *B. oleracea* plantlets resistant to *R. solani* in the initial phase of the pathogenesis. These results also show that a brief interaction (6 h) with *T. harzianum* ETS 323 is sufficient for the plant to develop resistance to *R. solani*-associated HS tissue damage.

**Rapid Induction of a GST and a DCD in the Resistant Tissues during the Three-Way Interaction Correlates with Damage Protection.** Cellular protective mechanisms to overcome stress include the activation of transcription factors, the repair of DNA damage, and increased expression of protective proteins such as antioxidant enzymes, glutathione (GSH), and heat shock proteins. Genes encoding many of these defense related products are also known to contain an electrophile response element/antioxidant response element and are therefore regulated by reactive molecules like hydroperoxides.[29]

Plant GSTs are a large and diverse group of antioxidant enzymes that catalyze the conjugation of electrophilic substrates with the GSH. They are involved in herbicide detoxification, hormone homeostasis, vacuolar sequestration of anthocyanin, tyrosine metabolism, hydroperoxide detoxification, regulation of apoptosis, and plant responses to biotic and abiotic stresses.[41] Further, binding of GSTs with various metabolites contributes to formation, stabilization, and transport of secondary metabolites and their intermediates. GSTs are known to be coregulated with enzymes of phytoalexin synthesis or enzymes synthesized in response to pathogens.[42] The BoGST expression in *B. oleracea* was activated during host HS response against *R.* solani and controlled the subsequent HS tissue damage. Cytotoxicity-related lipid peroxidation products, particularly hydroxyalkenals and isothiocyanates, are the natural substrates of GSTs in *Brassica* species. Therefore, the functions of GSTs include the development of resistance in cytotoxic conditions and more specifically to HS damage caused by LOX-derived electrophilic adducts.[30,43−47]

In plants, the early responses during the interaction with microbes include generation of active oxygen species related signaling molecules, such as $H_2O_2$ and $O_2^-$. These molecules are associated with several events occurring during the interaction with pathogens, such as acceleration of phenylpropanoid pathway and salicylic acid-related signaling.[48,49] At low concentrations $H_2O_2$ acts as signaling molecule that triggers biotic stress tolerance, while at high concentrations they cause PCD.[41] They also act as substrates for LOX-mediated jasmonic acid synthesis that is implicated with plant systemic resistance.[50]

In roots of *A. thaliana*, the association with unaggressive strains of *R. solani* is known to induce a localized expression of GSTF8, a GST that is $H_2O_2$ inducible.[51] The mechanism of expression of GST in *B. oleracea* herein reported is different, because the expression is systemic and depends on the combined effect of *R. solani* and *T. harzianum* ETS 323 interaction and not on either one of them solely. Interestingly, the GST induced during the three-way interaction was also induced by 30 mM $H_2O_2$. In this case GST was expressed systemically, unlike GSTF8 in *A. thaliana*.[51] These results suggest that the systemic expression of the GST requires

specific levels of relatively less toxic signaling molecules, such as $H_2O_2$, which are reached during the three-way interaction. Further, like most GSTs, the induced GST might neutralize the highly reactive peroxides produced during the incompatible interaction with *R. solani* and thus restrict the HS tissue damage.

Plant DCDs are nucleoside deaminases, with unknown physiological functions, that deaminates dCMP into dUMP. They have been well-studied in mammalian systems for their role in mutagenesis, cellular proliferation, lipid metabolism, and defense mechanism involving neutralization of cytotoxins.[52−56] Enhanced DCD expression has been previously reported in rice (*O. sativa*) during fungal interaction. It has been also postulated that the increase in DCD levels initiate an array of dynamic and complex transcript modifications that change the plant transcriptome and eventually enhance the host response during the early stages of fungal infection.[57] The DCD induction is an indicator of enhanced transcription regulatory activity during the three-way interaction. However, the significance of dC to dU conversion by the inducible DCD in DNA damage protection can also be extrapolated from the fact that the deoxycytidine in nucleosides and the dCTP in dsDNA are the main targets of LOX-related DNA adducts.[57−59] So far, no evidence is available to elucidate the role of DCD in plant resistance. The fact that the BoDCD, with a potential role in HS tissue damage control, is induced systemically during fungal interaction paves the way for further exploration. BoDCD, unlike BoGST, is not induced by $H_2O_2$, but the coexpression of the two genes during the three-way interaction emphasizes that the events occurring during the three-way interaction to ensue HS damage control are not limited to typical $H_2O_2$-mediated early plant response.

Our results reveal a novel mechanism of biocontrol of *R. solani* by *T. harzianum* ETS 323, in *B. oleracea*, based on the limitation of HS tissue damage. The mechanism for lesion control includes the expression of proteins induced by the three-way interaction, which results in the confinement of cell oxidation-related RES molecules and of the HS tissue damage. The induction of the antioxidant enzyme BoGST, by early signaling molecules of plant-microbe interaction, such as $H_2O_2$, facilitate the scavenging of cytotoxic adducts that damages cell macromolecules. The induced BoDCD potentially regulates the gene expression and neutralizes the cytotoxic DNA adducts and maintains the DNA integrity. The induced proteins can also be considered as molecular markers for enhanced stress tolerance or cellular protective mechanism against HS lesions in *B. oleracea*.

## AUTHOR INFORMATION


### Corresponding Author

*Telephone: +886 3 863 3635. Fax +886 3 863 3630. E-mail hhyang@tzuchi.com.tw, kcpeng@mail.ndhu.edu.tw.



### Funding

This work was partly supported by the grant from Buddhist Tzu-Chi General Hospital, Hualien, Taiwan (TCRD-I9801-03) and it is a part of the Ph.D. thesis of M.A. Shibu., who was financially supported by the Taiwan scholarship awarded by Ministry of Foreign Affairs of the Republic of China and from the Department of Life Science, National Dong Hwa University.


### Notes

The authors declare no competing financial interest.

## ACKNOWLEDGMENTS


We thank B. Y. Huang, H. N. Shih, and F. J. Tsai from K. C. Peng's laboratory and W. J. Zhai of H. H. Yang's Laboratory for all their help that facilitated this work.


## REFERENCES


(1) Sharma, H. C.; Crouch, J. H.; Sharma, K. K.; Seetharama, N.; Hash, C. T. Applications of biotechnology for crop improvement: Prospects and constraints. *Plant Sci.* **2002**, *163*, 381−395.

(2) Pearson, D. E.; Callaway, R. M. Indirect nontarget effects of host-specific biological control agents: Implications for biological control. *Biol. Control* **2005**, *35*, 288−298.

(3) Boland, G. J.; Brimner, T. Nontarget effects of biological control agents. *New Phytol.* **2004**, *163*, 455−457.

(4) Pannecoucque, J.; Hofte, M. Interactions between cauliflower and *Rhizoctonia anastomosis* groups with different levels of aggressiveness. *BMC Plant Biol.* **2009**, *9*.

(5) Gonzalez, M.; Pujol, M.; Metraux, J. P.; Gonzalez-Garcia, V.; Bolton, M. D.; Borras-Hidalgo, O. Tobacco leaf spot and root rot caused by *Rhizoctonia solani* Kuhn. *Mol. Plant Pathol.* **2011**, *12*, 209−16.

(6) Huang, X. Q.; Chen, L. H.; Ran, W.; Shen, Q. R.; Yang, X. M. *Trichoderma harzianum* strain SQR-T37 and its bio-organic fertilizer could control *Rhizoctonia solani* damping-off disease in cucumber seedlings mainly by the mycoparasitism. *Appl. Microbiol. Biotechnol.* **2011**, *91*, 741−755.

(7) Wilson, P. S.; Ketola, E. O.; Ahvenniemi, P. M.; Lehtonen, M. J.; Valkonen, J. P. T. Dynamics of soilborne *Rhizoctonia solani* in the presence of *Trichoderma harzianum*: Effects on stem canker, black scurf and progeny tubers of potato. *Plant Pathol.* **2008**, *57*, 152−161.

(8) Hanson, J. R. The chemistry of the bio-control agent, *Trichoderma harzianum*. *Sci. Prog.* **2005**, *88*, 237−48.

(9) Brotman, Y.; Lisec, J.; Meret, M.; Chet, I.; Willmitzer, L.; Viterbo, A. Transcript and metabolite analysis of the *Trichoderma*-induced systemic resistance response to *Pseudomonas syringae* in *Arabidopsis thaliana*. *Microbiology* **2012**, *158*, 139−46.

(10) Moran-Diez, E.; Rubio, B.; Dominguez, S.; Hermosa, R.; Monte, E.; Nicolas, C. Transcriptomic response of *Arabidopsis thaliana* after 24h incubation with the biocontrol fungus *Trichoderma harzianum*. *J. Plant Physiol.* **2012**, *169*, 614−20.

(11) Benitez, T.; Rincon, A. M.; Limon, M. C.; Codon, A. C. Biocontrol mechanisms of *Trichoderma* strains. *Int. Microbiol.* **2004**, *7*, 249−260.

(12) Marra, R.; Ambrosino, P.; Carbone, V.; Vinale, F.; Woo, S. L.; Ruocco, M.; Ciliento, R.; Lanzuise, S.; Ferraioli, S.; Soriente, I.; Gigante, S.; Turra, D.; Fogliano, V.; Scala, F.; Lorito, M. Study of the three-way interaction between *Trichoderma atroviride*, plant and fungal pathogens by using a proteomic approach. *Curr. Genet.* **2006**, *50*, 307−321.

(13) Liu, S. Y.; Lo, C. T.; Chen, C. P.; Liu, M. Y.; Chen, J. H.; Peng, K. C. Efficient isolation of anthraquinone-derivatives from *Trichoderma harzianum* ETS 323. *J. Biochem. Biophys. Methods* **2007**, *70*, 391−395.

(14) Yang, C. A.; Cheng, C. H.; Liu, S. Y.; Lo, C. T.; Lee, J. W.; Peng, K. C. Identification of antibacterial mechanism of L-amino acid oxidase derived from *Trichoderma harzianum* ETS 323. *FEBS J.* **2011**, *278*, 3381−3394.

(15) Yang, C. A.; Cheng, C. H.; Lo, C. T.; Liu, S. Y.; Lee, J. W.; Peng, K. C. A novel L-amino acid oxidase from *Trichoderma harzianum* ETS 323 associated with antagonism of *Rhizoctonia solani*. *J. Agric. Food Chem.* **2011**, *59*, 4519−4526.

(16) Llu, S. Y.; Shibu, M. A.; Jhan, H. J.; Lo, C. T.; Peng, K. C. Purification and characterization of novel glucanases from *Trichoderma harzianum* ETS 323. *J. Agric. Food Chem.* **2010**, *58*, 10309−10314.

(17) Kruger, N. J. The Bradford method for protein quantitation. *Methods Mol. Biol.* **1994**, *32*, 9−15.

(18) Ryerson, D. E.; Heath, M. C. Cleavage of nuclear DNA into oligonucleosomal fragments during cell death induced by fungal infection or by abiotic treatments. *Plant Cell* **1996**, *8*, 393−402.

(19) Gharahdaghi, F.; Weinberg, C. R.; Meagher, D. A.; Imai, B. S.; Mische, S. M. Mass spectrometric identification of proteins from silver-stained polyacrylamide gel: A method for the removal of silver ions to enhance sensitivity. *Electrophoresis* **1999**, *20*, 601−5.
(20) Tseng, S. C.; Liu, S. Y.; Yang, H. H.; Lo, C. T.; Peng, K. C. Proteomic study of biocontrol mechanisms of *Trichoderma harzianum* ETS 323 in response to *Rhizoctonia solani*. *J. Agric. Food Chem.* **2008**, *56*, 6914−22.
(21) Viterbo, A.; Harel, M.; Horwitz, B. A.; Chet, I.; Mukherjee, P. K. *Trichoderma* mitogen-activated protein kinase signaling is involved in induction of plant systemic resistance. *Appl. Environ. Microbiol.* **2005**, *71*, 6241−6246.
(22) Harman, G. E.; Howell, C. R.; Viterbo, A.; Chet, I.; Lorito, M. *Trichoderma* species—Opportunistic, avirulent plant symbionts. *Nat. Rev. Microbiol.* **2004**, *2*, 43−56.
(23) Chacon, M. R.; Rodriguez-Galan, O.; Benitez, T.; Sousa, S.; Rey, M.; Llobell, A.; Delgado-Jarana, J. Microscopic and transcriptome analyses of early colonization of tomato roots by *Trichoderma harzianum*. *Int. Microbiol.* **2007**, *10*, 19−27.
(24) Mariutto, M.; Duby, F.; Adam, A.; Bureau, C.; Fauconnier, M. L.; Ongena, M.; Thonart, P.; Dommes, J. The elicitation of a systemic resistance by *Pseudomonas putida* BTP1 in tomato involves the stimulation of two lipoxygenase isoforms. *BMC Plant Biol.* **2011**, *11*, 29.
(25) Marmey, P.; Jalloul, A.; Alhamdia, M.; Assigbetse, K.; Cacas, J. L.; Voloudakis, A. E.; Champion, A.; Clerivet, A.; Montillet, J. L.; Nicole, M. The 9-lipoxygenase GhLOX1 gene is associated with the hypersensitive reaction of cotton *Gossypium hirsutum* to *Xanthomonas campestris* pv *malvacearum*. *Plant Physiol. Biochem.* **2007**, *45*, 596−606.
(26) Rance, I.; Fournier, J.; Esquerre-Tugaye, M. T. The incompatible interaction between *Phytophthora parasitica* var. *nicotianae* race 0 and tobacco is suppressed in transgenic plants expressing antisense lipoxygenase sequences. *Proc. Natl. Acad. Sci. U. S. A.* **1998**, *95*, 6554−6559.
(27) Croft, K. P. C.; Voisey, C. R.; Slusarenko, A. J. Mechanism of hypersensitive cell collapse: Correlation of increased lipoxygenase activity with membrane damage in leaves of *Phaseolus vulgaris* (L) inoculated with an avirulent race of *Pseudomonas syringae* pv. *phaseolicola*. *Physiol. Mol. Plant Pathol.* **2004**, *36*, 49−62.
(28) Jalloul, A.; Montillet, J. L.; Assigbetse, K.; Agnel, J. P.; Delannoy, E.; Triantaphylides, C.; Daniel, J. F.; Marmey, P.; Geiger, J. P.; Nicole, M. Lipid peroxidation in cotton: *Xanthomonas* interactions and the role of lipoxygenases during the hypersensitive reaction. *Plant J.* **2002**, *32*, 1−12.
(29) Groeger, A. L.; Freeman, B. A. Signaling actions of electrophiles: Anti-inflammatory therapeutic candidates. *Mol. Interventions* **2010**, *10*, 39−50.
(30) Davoine, C.; Falletti, O.; Douki, T.; Iacazio, G.; Ennar, N.; Montillet, J. L.; Triantaphylides, C. Adducts of oxylipin electrophiles to glutathione reflect a 13 specificity of the downstream lipoxygenase pathway in the tobacco hypersensitive response. *Plant Physiol.* **2006**, *140*, 1484−93.
(31) Wilson, R. A.; Gardner, H. W.; Keller, N. P. Cultivar-dependent expression of a maize lipoxygenase responsive to seed infesting fungi. *Mol. Plant-Microbe Interact.* **2001**, *14*, 980−7.
(32) Parmeter, J. R. *Rhizoctonia solani, Biology and Pathology*; University of California Press: Berkeley, CA, 1970; p 255 p.
(33) Apel, K.; Hirt, H. Reactive oxygen species: Metabolism, oxidative stress, and signal transduction. *Annu. Rev. Plant Biol.* **2004**, *55*, 373−399.
(34) Ferreira, R. B.; Monteiro, S.; Freitas, R.; Santos, C. N.; Chen, Z.; Batista, L. M.; Duarte, J.; Borges, A.; Teixeira, A. R. The role of plant defence proteins in fungal pathogenesis. *Mol. Plant Pathol.* **2007**, *8*, 677−700.
(35) Skalamera, D.; Jibodh, S.; Heath, M. C. Callose deposition during the interaction between cowpea (*Vigna unguiculata*) and the monokaryotic stage of the cowpea rust fungus (*Uromyces vignae*). *New Phytol.* **1997**, *136*, 511−524.
(36) Huckelhoven, R. Cell wall-associated mechanisms of disease resistance and susceptibility. *Annu. Rev. Phytopathol.* **2007**, *45*, 101−127.
(37) Van Breusegem, F.; Dat, J. F. Reactive oxygen species in plant cell death. *Plant Physiol.* **2006**, *141*, 384−90.
(38) Laluk, K.; Mengiste, T. Necrotroph attacks on plants: wanton destruction or covert extortion? *Arabidopsis Book* **2010**, *8*, e0136.
(39) Howell, C. R.; Hanson, L. E.; Stipanovic, R. D.; Puckhaber, L. S. Induction of terpenoid synthesis in cotton roots and control of *Rhizoctonia solani* by seed treatment with *Trichoderma virens*. *Phytopathology* **2000**, *90*, 248−52.
(40) Kumar, V.; Parkhi, V.; Kenerley, C. M.; Rathore, K. S. Defense-related gene expression and enzyme activities in transgenic cotton plants expressing an endochitinase gene from *Trichoderma virens* in response to interaction with *Rhizoctonia solani*. *Planta* **2009**, *230*, 277−91.
(41) Gill, S. S.; Tuteja, N. Reactive oxygen species and antioxidant machinery in abiotic stress tolerance in crop plants. *Plant Physiol. Biochem.* **2010**, *48*, 909−30.
(42) Dixon, D. P.; Skipsey, M.; Edwards, R. Roles for glutathione transferases in plant secondary metabolism. *Phytochemistry* **2010**, *71*, 338−50.
(43) Kolm, R. H.; Danielson, U. H.; Zhang, Y.; Talalay, P.; Mannervik, B. Isothiocyanates as substrates for human glutathione transferases: Structure−activity. *Biochem. J.* **1995**, *311*, 453−459.
(44) Shapiro, T. A.; Fahey, J. W.; Wade, K. L.; Stephenson, K. K.; Talalay, P. Chemoprotective glucosinolates and isothiocyanates of broccoli sprouts: Metabolism and excretion in humans. *Cancer Epidemiol., Biomarkers Prev.* **2001**, *10*, 501−8.
(45) Kampranis, S. C.; Damianova, R.; Atallah, M.; Toby, G.; Kondi, G.; Tsichlis, P. N.; Makris, A. M. A novel plant glutathione S-transferase/peroxidase suppresses Bax lethality in yeast. *J. Biol. Chem.* **2000**, *275*, 29207−29216.
(46) Sappl, P. G.; Onate-Sanchez, L.; Singh, K. B.; Millar, A. H. Proteomic analysis of glutathione S-transferases of *Arabidopsis thaliana* reveals differential salicylic acid-induced expression of the plant-specific phi and tau classes. *Plant Mol. Biol.* **2004**, *54*, 205−19.
(47) Blair, I. A. DNA adducts with lipid peroxidation products. *J. Biol. Chem.* **2008**, *283*, 15545−15549.
(48) Tang, M.; Smith, C. J. Elicitor induced defence responses in *Medicago sativa*. *New Phytol.* **2001**, *149*, 401−418.
(49) Heil, M.; Bostock, R. M. Induced systemic resistance (ISR) against pathogens in the context of induced plant defences. *Ann. Bot.* **2002**, *89*, 503−512.
(50) Benhamou, N. Elicitor-induced plant defence pathways. *Trends Plant Sci.* **1996**, *1*, 233−240.
(51) Perl-Treves, R.; Foley, R. C.; Chen, W.; Singh, K. B. Early induction of the *Arabidopsis* GSTF8 promoter by specific strains of the fungal pathogen *Rhizoctonia solani*. *Mol. Plant−Microbe Interact.* **2004**, *17*, 70−80.
(52) Neff, T.; Blau, A. Forced expression of cytidine deaminase confers resistance to cytosine arabinoside and gemcitabine. *Exp. Hematol.* **1996**, *24*, 1340−1346.
(53) van Beerendonk, G. J.; van Gog, F. B.; Vrieling, H.; Pearson, P. G.; Nelson, S. D.; Meerman, J. H. Blocking of in vitro DNA replication by deoxycytidine adducts of the mutagen and clastogen 2-bromoacrolein. *Cancer Res.* **1994**, *54*, 679−84.
(54) Bransteitter, R.; Prochnow, C.; Chen, X. J. S. The current structural and functional understanding of APOBEC deaminases. *Cell. Mol. Life Sci.* **2009**, *66*, 3137−3147.
(55) Conticello, S. G.; Langlois, M. A.; Yang, Z.; Neuberger, M. S. DNA deamination in immunity: AID in the context of its APOBEC relatives. *Adv. Immunol.* **2007**, *94*, 37−73.
(56) Gowda, M.; Venu, R. C.; Li, H.; Jantasuriyarat, C.; Chen, S.; Bellizzi, M.; Pampanwar, V.; Kim, H.; Dean, R. A.; Stahlberg, E.; Wing, R.; Soderlund, C.; Wang, G. L. *Magnaporthe grisea* infection triggers RNA variation and antisense transcript expression in rice. *Plant Physiol.* **2007**, *144*, 524−33.

(57) Olsen, R.; Molander, P.; Ovrebo, S.; Ellingsen, D. G.; Thorud, S.; Thomassen, Y.; Lundanes, E.; Greibrokk, T.; Backman, J.; Sjoholm, R.; Kronberg, L. Reaction of glyoxal with 2′-deoxyguanosine, 2′-deoxyadenosine, 2′-deoxycytidine, cytidine, thymidine, and calf thymus DNA: Identification of DNA adducts. *Chem. Res. Toxicol.* **2005**, *18*, 730−9.

(58) Pollack, M.; Oe, T.; Lee, S. H.; Silva Elipe, M. V.; Arison, B. H.; Blair, I. A. Characterization of 2′-deoxycytidine adducts derived from 4-oxo-2-nonenal, a novel lipid peroxidation product. *Chem. Res. Toxicol.* **2003**, *16*, 893−900.

(59) Kawai, Y.; Uchida, K.; Osawa, T. 2′-Deoxycytidine in free nucleosides and double-stranded DNA, as the major target of lipid peroxidation products. *Free Radical Biol. Med.* **2004**, *36*, 529−541.

## ■ NOTE ADDED AFTER ASAP PUBLICATION

Figure 7 was modified in the version of this paper published October 19, 2012. The correct version published October 22, 2012.